

## Space-Diversity Engineering

By A. VIGANTS

(Manuscript received March 14, 1974)

*Vertically separated antennas are recommended to increase the transmission availability of line-of-sight microwave links by reducing the duration and frequency of multipath fading events. The emphasis is on application to the 4- and 6-GHz bands on links with negligible ground reflections. Necessary signal processing, links utilizing passive repeaters (reflectors), and overwater links are also treated. Some new experimental data are presented.*

### I. INTRODUCTION

Bell System microwave radio relay routes consist of links (paths, hops) that have an average length of about 26 miles. Transmission on most hops is along the line of sight, with antennas mounted on towers that are typically 250 feet high. In some cases, when line-of-sight transmission between towers is not practical, large reflectors on prominent points of terrain (passive repeaters) are used. Tower locations are selected to avoid ground reflections, but inevitable exceptions, such as transmission across a lake, do occur.

Multipath propagation during anomalous atmospheric conditions can give rise to destructive interferences at the receiving antenna; the resultant signal fluctuates (fades) and may be reduced to practically zero for seconds at a time. The corresponding interruptions to service, if permitted to occur, would be unacceptable. Interruptions to operation can be avoided by switching from an unserviceable radio channel to a protection channel operating at a different radio frequency, since multipath fading, being an interference phenomenon, is frequency selective. Use of such protection (frequency diversity) has been restricted to conserve the frequency spectrum.<sup>1</sup>

Space diversity is an alternative or additional form of protection from the effects of multipath fading.<sup>2-8</sup> Its effectiveness depends upon the fact that multipath propagation results in vertical structure of the electromagnetic fields at the receiving tower. Selection between two vertically separated antennas receiving at the same frequency is com-

parable in effect to a frequency-diversity system with a protection channel for every working channel (switched on a per-hop basis). Unfamiliarity with the principles of operation and unavailability of space-diversity equipment, as well as costs, have inhibited use of space diversity in the past. Currently, use of space diversity is increasing. One reason for this (apart from spectrum conservation) is that, in areas of high fading, frequency diversity alone cannot provide the desired transmission availability.

Space-diversity engineering, as presented here, encompasses estimation of fading, determination from transmission availability objectives of the need for protection, and calculation of the antenna separation needed to obtain the required transmission availability. The effects of signal processing on the improvement available from an antenna pair are discussed, with particular attention given to threshold switching. Space diversity through passive repeaters and on over-water paths is also discussed. Clearance requirements are summarized in the last section; current work on antennas placed so low as to lack clearance under normal propagation conditions is discussed in Appendix A.

The emphasis in this paper is on application in the 4- and 6-GHz frequency bands, although the expressions for the estimation of the amount of fading and the diversity improvement apply to other microwave frequencies. However, transmission in the 11-GHz band is also affected by rain, and this must be taken into account by additional reduction of the effects of multipath fading. This design aspect belongs more properly in a treatment of 11-GHz radio system design and is not discussed here.

## II. DESCRIPTION OF FADING

The RF power received after transmission over a microwave radio hop is never absolutely constant; even at noon, when the atmosphere has "stabilized," there can be fractional dB excursions (scintillations recurring a few times per second), as well as slower excursions of a dB or two. In propagation experiments, the normal value of the received signal is determined from the peak in a signal-level histogram obtained over at least one-half hour at or near noon. This so-called free-space value of the received signal is determined repeatedly at least once a week to identify periods during which enhanced or depressed signals have resulted from the relatively steady atmospheric focusing or defocusing. These periods, therefore, are not "normal."

During fading, the received RF power can be practically zero for seconds at a time. The terminology to describe this is introduced in Fig. 1 through an example in which the free-space value is  $-30$  dBm and a single, idealized fade decreases the received power temporarily

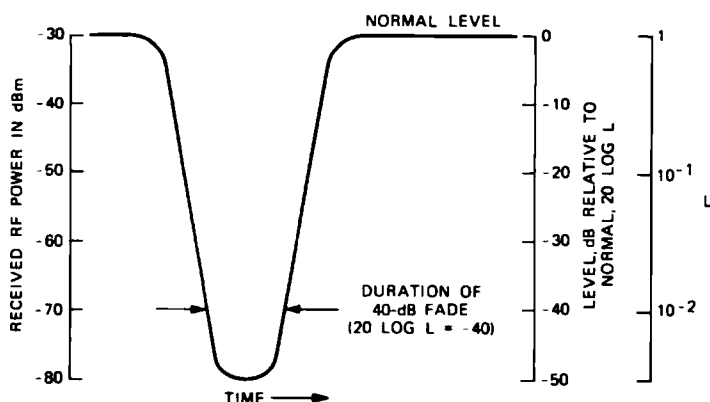


Fig. 1—Definitions of  $L$  and fade duration ( $-30$  dBm assumed normal as an example).

to  $-80$  dBm; levels in dB relative to normal are denoted by  $20 \log L$ . The time during which a signal is below a level is called the duration of fade of that level (the duration of a 40-dB fade is illustrated in Fig. 1). Average durations of fades are independent of microwave frequency\* and are proportional to  $L$ ; typical numerical values are given by (see also Fig. 2)<sup>9-11</sup>

$$\langle t \rangle = 410 L \text{ seconds, } L < 0.1. \quad (1)$$

As an example, the average duration of a 40-dB fade ( $L = 10^{-2}$ ) is 4.1 seconds, both at 4 and 6 GHz.

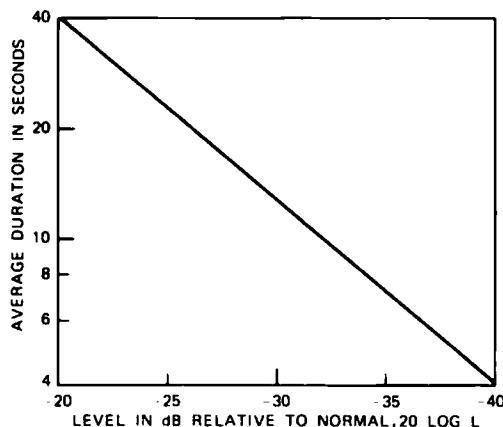


Fig. 2—Average fade durations ( $\langle t \rangle = 410L$ ,  $L < 0.1$ ).

\* An underlying assumption throughout this work is that antenna sizes and path lengths are as encountered most often in practice: antenna diameters are between about 4 and 16 feet, and path lengths are between about 14 and 40 miles.

The sum of the durations of all fades of a particular depth is called "time below level." It is proportional to  $L^2$ , since the number of fades is proportional to  $L$ , and its numerical values are given by<sup>9</sup>

$$T = rT_0L^2, \quad L < 0.1, \quad (2)$$

where  $T_0$  is the time period over which the summation of fade durations is made (a month, for example); the units of  $T$  are those of  $T_0$  (seconds are normally used). The fade occurrence factor  $r$  for heavy fading months (see Fig. 3) is<sup>9</sup>

$$r = c(f/4)D^2 10^{-5}, \quad (3)$$

where

$$\begin{aligned} c &= 4 \text{ over water and Gulf coast,} \\ &= 1 \text{ average terrain and climate,} \\ &= \frac{1}{4} \text{ mountains and dry climate,} \\ f &= \text{frequency in GHz,} \end{aligned} \quad (4)$$

and

$D$  = path length in miles.

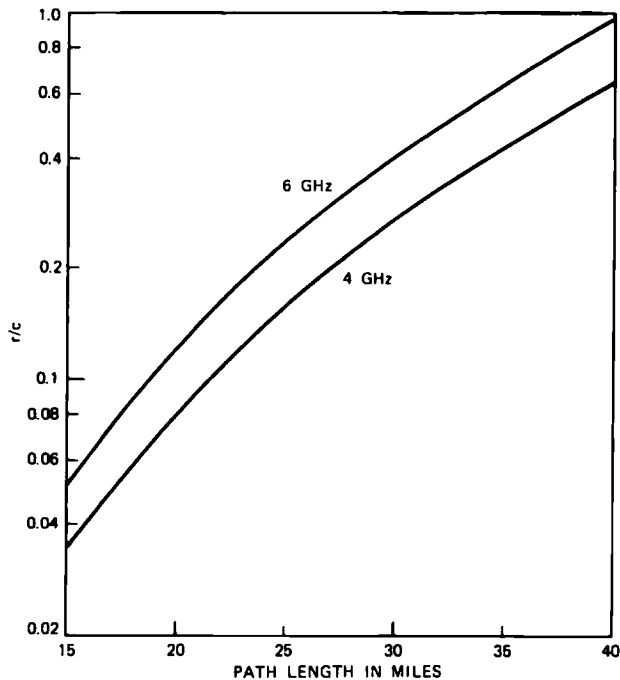


Fig. 3—Multipath occurrence factor.

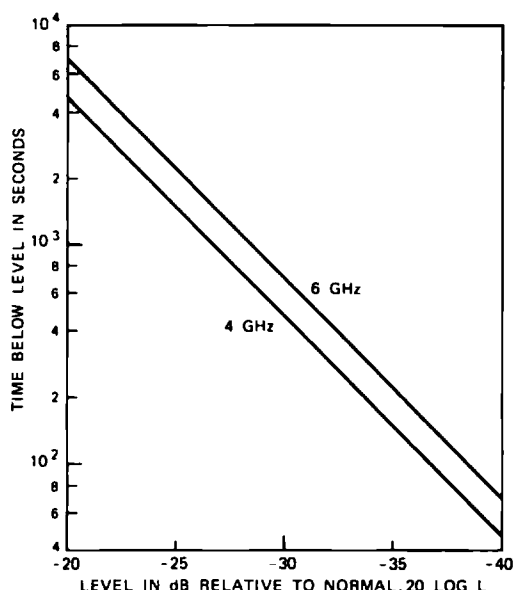


Fig. 4—Time below level in a heavy fading month ( $D = 26$  miles,  $c = 1$ ,  $T_0 = 31$  days  $= 2.68 \times 10^6$  seconds).

As an example, values of  $T$  as a function of fade depth for a 26-mile path (average length) and average terrain and climate are shown in Fig. 4 for a heavy fading month. The lines have the decade of time per 10-dB slope typical of multipath fading, specified by the  $L^2$  functional dependence. The values of  $T$  at  $-40$  dB are 47 and 71 seconds at 4 and 6 GHz, respectively. Based on an average duration of 4.1 seconds, this corresponds to 11 fades of 40 dB at 4 GHz.

The coefficient  $c$  in (4) incorporates the effects of both terrain and humidity and is adequate for first estimates of expected fading in many cases. Differentiation between paths of identical climate but differing terrain can be done by introducing a terrain roughness parameter<sup>12</sup> quantifying common knowledge that paths over rough terrain fade less than paths over smooth terrain, presumably because stable atmospheric layering is less likely to occur over rough terrain. Terrain roughness is calculated from terrain heights above a reference level (sea level, for example) obtained from the path profile at one-mile intervals, with the ends of the path excluded. The standard deviation of the resulting set of numbers is the terrain roughness, denoted by  $w$  (see sample calculation in Appendix B). Applicable values of  $w$  range from 20 feet ("smooth") to 140 feet ("rough"); values of 20 and 140 should be used when calculated values of  $w$  are less than 20 or larger than 140.

Modified for roughness, the equations for  $c$  become:

$$\begin{aligned} c &= 2 (w/50)^{-1.3}, \text{ coastal areas,} \\ &= (w/50)^{-1.3}, \text{ average climate,} \\ &= 0.5 (w/50)^{-1.3}, \text{ dry climate,} \end{aligned} \tag{5}$$

where a roughness of 50 feet has been defined as "normal."

### III. PERFORMANCE OBJECTIVES

The time below level of the received signal, at a fade depth equal to the receiver fade margin, represents potential service-failure time. Protection is needed if this exceeds the value set by transmission-availability objectives.

Bell System short-haul objectives limit service failure time to 0.02 percent (two-way) annually on a 250-mile route due to all causes. One-half of this is allocated to causes associated with equipment, maintenance, and plant errors. There are obvious exceptions to this; for example, unavailability on a route where all hops are exceptionally short will be due mainly to equipment outages, and may be so allocated.

The allocation to fading, therefore, is 0.01 percent (two-way) annually. In the past, this allocation had been apportioned between multipath and obstruction fading ("earth-bulge" fading). However, the occurrence of intolerable obstruction fading can be decreased by increasing clearance (higher towers or shorter hops) or by increasing system gain margin; reliability records show that there has been a gradual decrease in the occurrence of obstruction fading over the years.<sup>18</sup> In the construction of new hops or in the upgrading of older ones in locations where obstruction fading is known to occur (or by related experience is expected to occur), increased clearances (or limits on path lengths) are assumed to be used. Consequently, no allocation to obstruction fading is made in space-diversity engineering; the entire 0.01 percent two-way annual fading allocation is applied to multipath fading. The one-way annual multipath fading allocation for 250 miles becomes 0.005 percent or approximately 26 minutes per year (1600 seconds per year). The corresponding allocation to a hop  $D$  miles long is  $1600 \times D/250$  seconds per year (165 seconds per year for the average 26-mile hop).

Estimated annual time below level (for comparison with the objective) is obtained from the equation for  $T$  in the previous section, with  $T_0$  describing the length of the fading season. As a geographic average, the value of  $T_0$  in this estimate is equal to the number of seconds in three months; this assumes that all significant fading is contained in two heavy and two medium fading months, which is equivalent to

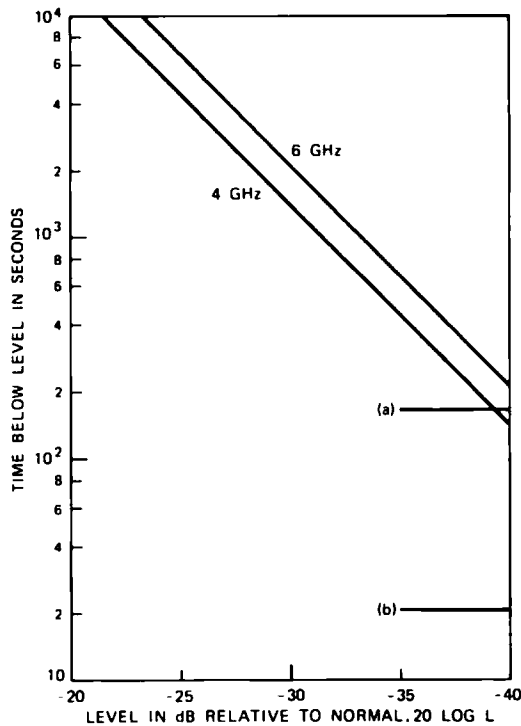


Fig. 5—Annual time below level (average case). Objectives: (a) short haul = 165 seconds/year, (b) long haul = 20 seconds/year.

three heavy fading months.<sup>14</sup> Estimation of the length of the fading season as a function of geographic location is discussed in Appendix C.

Continuation of the example of Fig. 4 provides the annual time-below-level curves in Fig. 5 (142 and 212 seconds below  $-40$  dB at 4 and 6 GHz, respectively). For a fade margin of 35 dB, considered here for the purposes of discussion, the time below level is too large, compared to the 165-second objective, by factors of 2.7 and 4 at 4 and 6 GHz, respectively; protection against multipath fading (space or frequency diversity) is needed when the fade margin is 35 dB. At a fade margin of 40 dB, the 4-GHz channel in the example can get by without protection.

For long-haul radio the overall objective is also 0.02 percent, but the route length is 4000 miles. However, long-haul transmission models assume that half of the hops never experience significant fading.<sup>14</sup> With the addition of this assumption to those previously made in this section, the long-haul multipath allocation to a hop  $D$  miles long becomes  $1600 \times D/2000$  seconds per year (20 seconds per year for the average 26-mile hop). In practice, long-haul radio has at least one protection

channel, which is required for equipment protection and maintenance and is used to provide frequency-diversity protection. Such use modifies the need for space-diversity protection (see Appendix D). Use of frequency diversity in short-haul radio can be expected to be infrequent because of regulatory restrictions.<sup>1</sup>

#### IV. THE SPACE-DIVERSITY EFFECT

During periods of multipath fading, deep fades of signals received on two vertically separated receiving antennas rarely overlap in time. The relatively few that do overlap give rise to simultaneous time below level (sum of durations of simultaneous fades, see Fig. 6), which is proportional to  $L^4$  and can be expressed as<sup>7,8,15</sup>

$$T_s = T/I_0, \quad (6)$$

where  $T$  is the time below level of the signal received on the main antenna and  $I_0$  is the available improvement, given numerically in practical units by the following (see also nomogram in Fig. 7):<sup>7,8</sup>

$$I_0 = 7 \times 10^{-5} v^2 s^2 f / DL^2, \quad s \leq 50, \quad (7)$$

where

$v$  = relative gain parameter (gain of secondary antenna relative to main antenna in dB is  $20 \log v$ ),

$s$  = vertical separation of receiving antennas in feet, center-to-center,

$f$  = frequency in GHz,

$D$  = path length in miles,

and

$L$  = level parameter (level in dB relative to normal is  $20 \log L$ ).

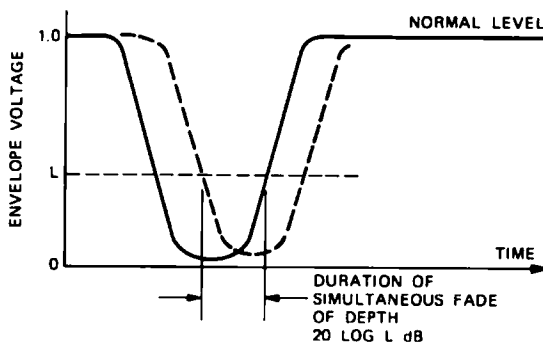


Fig. 6—Definition of simultaneous fade.



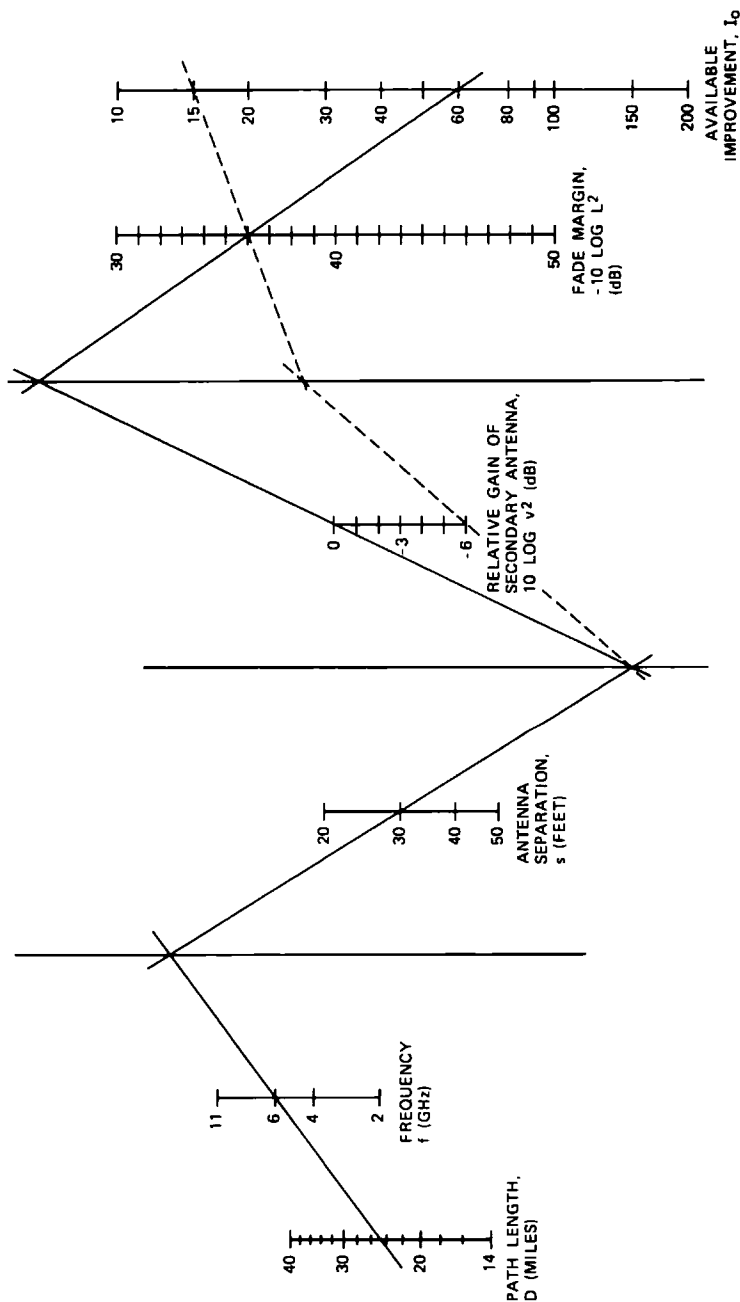


Fig. 7—Nomogram for available improvement  $I_o$ .

Equation (7) applies only for the ranges of variables indicated on the nomogram in Fig. 7. Extrapolation of the scales may lead to errors. For example, under some conditions the increase in improvement due to an increase in separation over 50 feet may be small. Separations for which the available improvement is less than 10 should not be used; if possible, separations of at least 30 feet should be used.

The example of Fig. 5 is continued in Fig. 8 to demonstrate drawing of a curve for  $T_s$ ; the secondary antenna in the example has the same gain as the main antenna ( $v^2 = 1$ ) and the vertical center-to-center separation of the antennas is 30 feet ( $s = 30$ ). The values of  $I_0$  at  $-40$  dB are 145 and 97 for the 6- and 4-GHz channels, respectively. The values of  $T_s$  at  $-40$  dB are  $212/145 = 1.46$  seconds and  $142/97 = 1.46$  seconds, identical for 6 and 4 GHz. This comes about because both  $T$  and  $I_0$  are proportional to frequency. Having established one point (1.46 seconds at  $-40$  dB) for  $T_s$ , we draw through it a line with a slope of a decade of time per 5 dB, as specified by the  $L^4$  functional dependence. When  $I_0$  becomes less than about 5, terms in addition to that proportional to  $L^4$  are needed to describe  $T_s$ , which is why the line for  $T_s$  in Fig. 8 is not extended all the way to the left into the region (normally not of practical interest) where  $T_s$  approaches  $T$ .

The simultaneous time below level in Fig. 8 is smaller than the 165-seconds-per-year short-haul objective for fade margins larger than about 30 dB; it is smaller than the 20-seconds-per-year long-haul objective for fade margins larger than about 34 dB.

## V. COMPARISON OF SPACE AND FREQUENCY DIVERSITY

Space diversity in its most common form provides a protection channel for every working channel ( $1 \times 1$  protection) on a per-hop basis. Frequency diversity usually provides one or two protection channels for  $m$  working channels ( $1 \times m$  or  $2 \times m$  protection) on the basis of switching sections that can contain as many as 10 hops in extreme cases. The most effective form of frequency diversity is, of course,  $1 \times 1$  on a per-hop basis (now restricted in use at 4 and 6 GHz because of spectrum conservation); this can readily be compared to space diversity.

For equal performance the available improvements,  $I_0$ , are equated. A convenient form for  $I_0$  is

$$I_0 = v^2 q L^{-2}, \quad (8)$$

where for space diversity (from the previous section)

$$q = 7 \times 10^{-5} s^2 f / D, \quad s \leq 50 \quad (9)$$

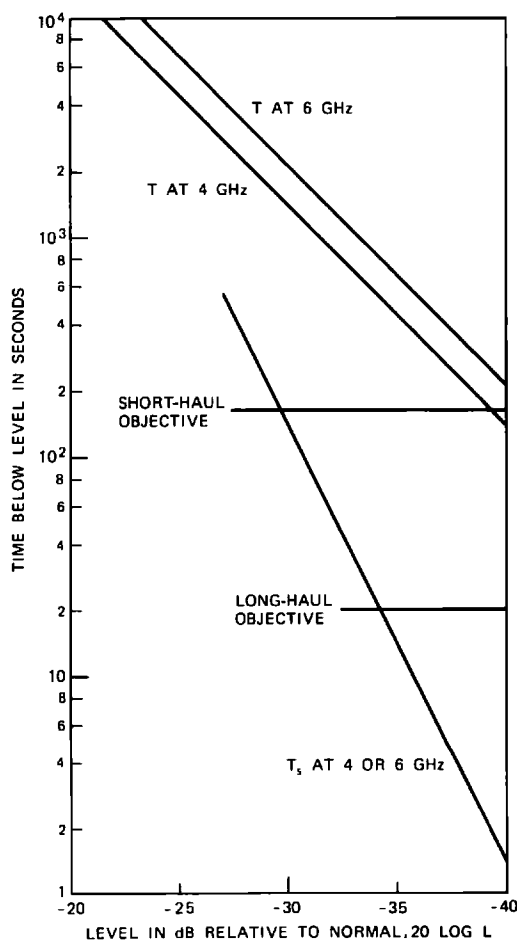


Fig. 8—Annual simultaneous time below level for 30-foot separation of antennas (continuation of average-case example from Fig. 5).

and for frequency diversity<sup>16</sup>

$$q = 50(\Delta f/f)/fD, \quad \Delta f < 0.5 \text{ GHz}, \quad (10)$$

where  $f$  is the frequency in GHz (4 or 6), and  $\Delta f$  is the difference of radio channel center frequencies, also in GHz;  $D$  is the path length in miles. Values of separations in space and frequency providing equal performance (for antennas of equal size;  $v^2 = 1$ ) are obtained by eliminating  $q$  from (9) and (10):

$$\begin{aligned} s &= 106 \sqrt{\Delta f}, \text{ in the 4-GHz band,} \\ &= 57.5 \sqrt{\Delta f}, \text{ in the 6-GHz band,} \end{aligned} \quad (11)$$

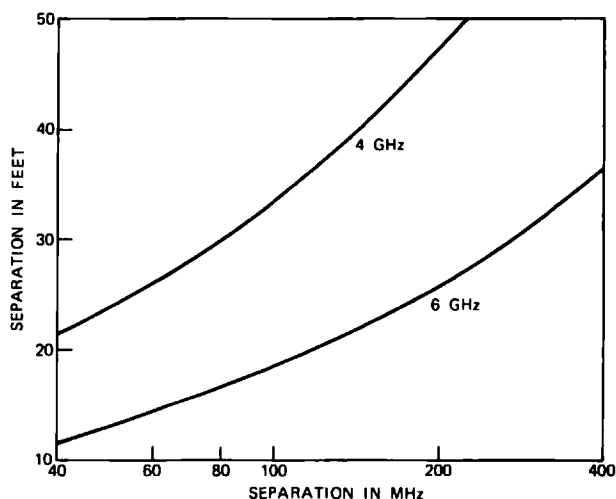


Fig. 9—Separations in space and frequency providing equal protection (one-for-one switching on a per-hop basis; antennas of equal size,  $v^2 = 1$ ).

where  $s$  is in feet. A 30-foot separation is equivalent to a  $\Delta f$  of about 0.08 GHz in the 4-GHz band and about 0.27 GHz in the 6-GHz band (Fig. 9).

## VI. SIGNAL PROCESSING

The signals received by the two antennas must be processed to obtain a diversity signal. Static addition at RF is not practical, since the duration of one-half cycle at, say, 4 GHz is  $\frac{1}{8}$  nanosecond, and delay changes of this magnitude in the relative arrival times of the two signals arise easily because of daily angle-of-arrival variations. Without dynamic phase compensation, such changes would lead to signal cancellations during normal daytime operation, even when multipath fading is not present. The cost of dynamic phase compensation has so far been prohibitive.

Addition at baseband without dynamic phase compensation has been used (duration of a half cycle at 10 MHz is 50 nanoseconds). In some implementations, the weaker signal is dropped from the sum, when the relative signal strength ratio exceeds some 4 dB, to improve the signal-to-noise ratio of the diversity signal. Simultaneous time below level can be used to approximate the time below level of the diversity signal.

Switching, particularly at RF, permits an economically advantageous configuration of equipment. The simultaneous time-below-level curves (Fig. 8) describe the performance of an idealized comparator (switch),

where the diversity signal is, at every instant, the stronger of the two received signals. The switching activity, accompanied by undesirable step phase changes, is high. This can be reduced by introducing hysteresis, but at the cost of reduced performance. Suppose switching occurs only when the ratio of the received powers is larger than a number  $b^2$  ( $10 \log b^2$  in dB). The improvement realized becomes

$$I = \eta I_0, \quad (12)$$

where an estimate of the efficiency factor  $\eta$  (see Appendix E) is

$$\eta = 2/(b^2 + b^{-2}). \quad (13)$$

As an example, when  $10 \log b^2$  is 6 dB,  $\eta$  is 0.47, and an available improvement of 100 becomes a realized improvement of 47.

A different approach must be used when only one receiver per radio channel is available, which is the case in long-haul radio. The diversity implementation utilizes an RF waveguide switch activated by the AGC voltage when the receiver input falls below a threshold (one example of switching logic is shown in Table I). Switching of this sort has been referred to as threshold or "blind" switching, since at the instant of switching there is no assurance that a stronger signal will be available at the other antenna. Most of the time, a stronger signal is found, since few of the deep fades on the two receiving antennas overlap in time. The time below level  $T_t$  for threshold switching is calculated (see Appendix F) in Fig. 10 for a 4-GHz channel (in continuation of the example from Fig. 8); the threshold is at  $-35$  dB relative to normal. The values of  $T_t$  and  $T_s$  are identical at the threshold. Above threshold,  $T_t$  approaches  $T$  rapidly, since the switch does not act for fades during which the minimum signal does not drop below  $-35$  dB. The part of  $T_t$  of importance in space-diversity engineering is the straight-line section below threshold. This straight-line section is parallel to  $T$ , since it represents an average of the two single-antenna statistics by virtue of the continued cycling of the switch due to failure

Table I — Switching logic of a threshold switch

Switch Output Relative to Switch Threshold	Switch Connected to	Action
High	Main antenna	Stay on main antenna
High	Secondary antenna	Switch to main antenna after 15 minutes
Low	Main antenna	Switch to secondary antenna after 0.1 second
Low	Secondary antenna	Switch to main antenna after 0.1 second

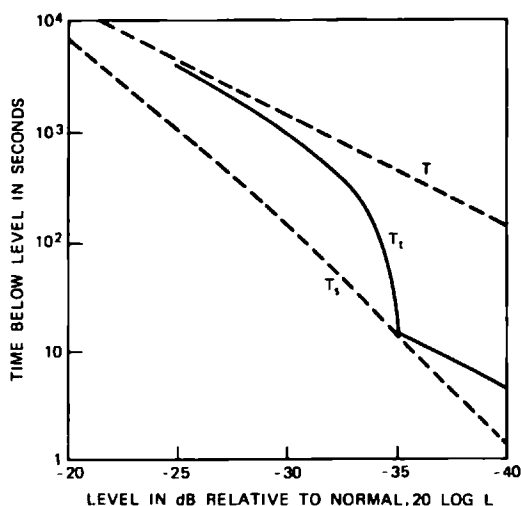


Fig. 10—Time below level in threshold switching—continuation of average-case example (4 GHz, threshold at  $-35$  dB, 30-foot separation of antennas).

of the receiver to locate a signal stronger than the threshold value, which is  $-35$  dB relative to normal in the example.

A suitable value of the threshold is about 2 dB above the fade margin. The  $-35$  dB threshold in the example would be appropriate for a fade margin of 37 dB. The improvement ( $I_i = T/T_i$ ) is constant below threshold (about 30 in the example) and equal to the value of  $I_0$  at

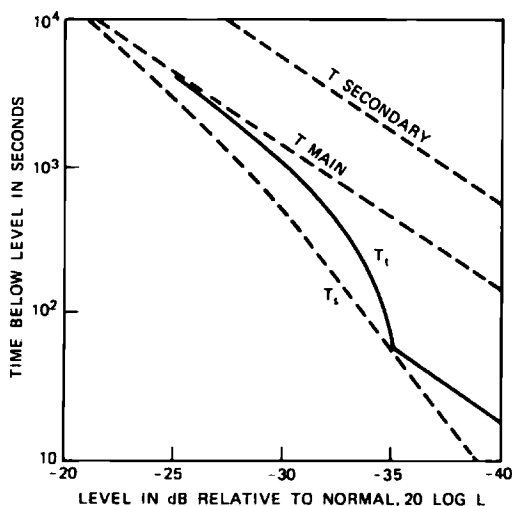


Fig. 11—Example of reduced performance due to smaller secondary antenna ( $10 \log v^2 = -6$ , other parameters as in Fig. 10).

the threshold. This is one reason for placing the threshold close to the fade margin, since a threshold at  $-30$  dB, for example, would provide an  $I_t$  of only about 10. A second reason is to limit the occurrence of the phase steps due to the cycling of the switch to occasions when the signals border on the unusable (actually, the chance is small that the signals remain for prolonged periods in the 2-dB corridor between the threshold and the fade margin, and many of the phase steps will occur, therefore, when the signals are unusable). The cycling should occur at a rate of at least five times per second; at much slower rates, a good signal is not found fast enough and performance deteriorates. Corridors smaller than 2 dB should be avoided, since signal drifts caused by aging of equipment or noise accumulation from hop to hop in a switching section can frustrate design intentions and require frequency diversity action before space diversity.

Use of a smaller secondary antenna reduces performance, as illustrated in Fig. 11, where the only change from Fig. 10 is that a secondary antenna with 6 dB less gain ( $v^2 = 0.25$ ) has been used. The improvement  $I_t$  has decreased to about 8 ( $\approx 30/4$ ) from about 30 in the equal-size-antenna case.

## VII. SPACE-DIVERSITY TRANSMISSION

Space diversity for microwave radio is usually envisioned as diversity reception; i.e., the system consists of a single antenna which transmits to two vertically separated receiving antennas. Since the path loss from antenna to antenna does not depend on the direction of transmission, an arrangement of two vertically separated transmitting antennas and a single receiving antenna can also be used.

Combined use of transmitting and receiving diversity can reduce tower work; on a long route only alternate towers would be affected. A single bad hop can be corrected by additional installation at one end only. On hops where additional installation at one end is impossible because of economics or zoning, use of both transmitting and receiving diversity at the other end provides full diversity protection in both directions.

A drawback to transmitting diversity is the vulnerability of the control signal. In diversity reception, the signals from both antennas are always available at the switching site, to be processed in any desired manner. In transmitting diversity, only one antenna can transmit at a given frequency at a given time (dynamic phase correction for control of the two transmitters does not appear feasible or desirable). The required control information must be fed back from the receiving to the transmitting end, since control must be based—because of the frequency selectivity of deep fades (see Appendix G)—on fading in

the controlled channel. The feedback link increases both the cost of control and the possibility for failure of control.

## VIII. FIELD EXPERIENCE

The basic experimental data on simultaneous fading on vertically separated receiving antennas were obtained in Ohio and Texas in 1966. The variation of the improvement as the square of the vertical separation of the antennas was further verified experimentally in Georgia in 1968 (Appendix H). Field followup in terms of monitoring performance of in-service space diversity was carried out in 1972 in California and Florida. The monitoring was made possible by the development of Portable Propagation Recorders (PPR), the first installation of which was at Brawley, California, in May 1972.

Space diversity in the California case was installed by Pacific Telephone and Telegraph Co. to improve transmission availability of two hops (Salton-Brawley and Brawley-Glamis traversing Imperial Valley) on the Dallas-Los Angeles route. Extensive irrigation and high temperatures with little wind combine to create severe fading on the two hops in question. Measured and calculated values of  $I_0$  are compared in Table II (Fig. 12 is an example of measured data). RF threshold switching was used, and the comparison was made at the threshold value ( $-35$  dB relative to normal) where  $I_c$  and  $I_0$  are equal.<sup>17</sup> The agreement of calculated and measured values is good, showing that the equation for  $I_0$  is applicable under diverse climatic conditions.

Two hops monitored in Florida (Andytown South-Andytown North and Andytown North-Okeelanta in Northern Everglades) were equipped with secondary receiving antennas and RF threshold switches as part of a program to improve transmission availability of hops that fade heavily. The measured results and the predictions for Andytown

Table II — Comparison of calculated and measured values of  $I_0$  (Salton-Brawley and Brawley-Glamis, California)\*

Antenna Spacing (feet)	Frequency (GHz)	Path Length (miles)	Relative Gain of Secondary Antenna ( $v^2$ )	$I_0$ at $20 \log L = -35$	
				Calculated from Equation (7)	Measured
30	4	42.6	0.41	7.6	8.0†
15	4	42.6	0.41	1.9	1.5‡
15	4	37.1	0.41	2.2	2.5§

\* Antenna configurations were dictated by circumstances; generally, configurations providing an improvement of at least 10 would be used.

† Brawley to Glamis, 7/7-8/14, 1972.

‡ Glamis to Brawley, 5/11-7/3, 7/7-8/14, 1972.

§ Salton to Brawley, 8/17-8/29, 1972.



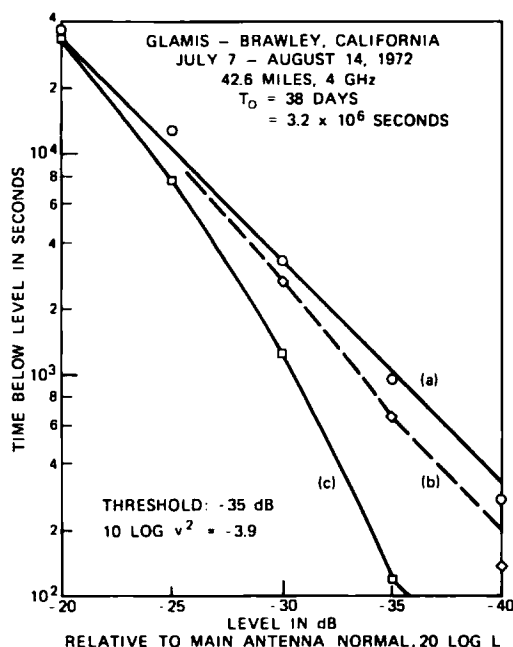


Fig. 12—Threshold switching, Glamis to Brawley, California. Reception at (a) Glamis, main antenna (unprotected), (b) Brawley, 15-foot separation, (c) Glamis, 30-foot separation.

South to Andytown North are summarized in Fig. 13.<sup>18</sup> At  $-47 \text{ dB}$  (bottom level of the PPR for this case), the predicted time below level in the 148-day test period was insignificant (only a few seconds), and none was measured. Diversity performance thus conformed to expectations and the needed improvement in transmission availability was obtained.

## IX. PATHS WITH PASSIVE REPEATERS

Use of passive repeaters (large reflectors of, say, 40 by 48 feet) on ridges or hilltops is sometimes dictated by terrain or by the undesirability of active repeaters in remote locations (power and maintenance-access problems). Tests on a Mountain Bell hop (Lusk-Wendover, Wyoming) in 1973 established that space diversity is operative through passive repeaters.<sup>19</sup> A design procedure for practical cases, based on the Wyoming results, is:

- (i) Determine reflector size to obtain reasonable fade margin.
- (ii) Estimate unprotected time below level ( $T$ ) as the sum of the values of  $T$  for the individual legs (distances from reflector to ends of hop).

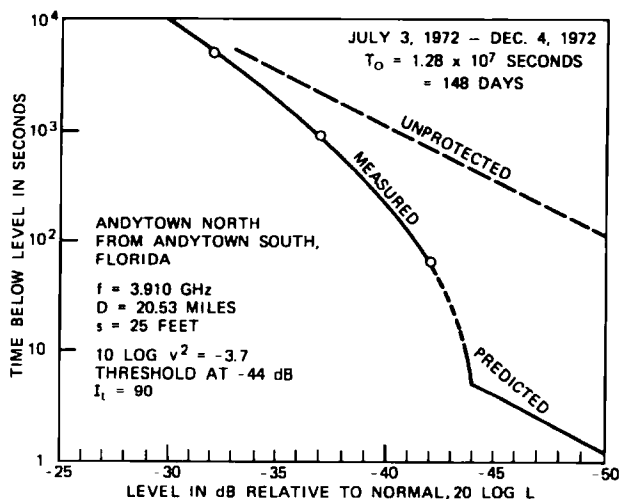


Fig. 13—Threshold switch operation at Andytown North, Florida.

- (iii) Determine improvement needed to meet transmission availability objectives.
- (iv) If improvement is needed, determine vertical spacing based on longest leg (use at least 20 or 30 feet); use this vertical spacing at both ends of hop.
- (v) If an antenna pair is in the near field of a reflector, ensure that projected reflector height is not less than the distance from the bottom edge of the bottom antenna to the top edge of the top antenna.

The experimental data obtained at Wendover and Lusk are summarized in Figs. 14 and 15 (the parameters of the experiment are summarized in Table III).<sup>19</sup> Time-below-level differences for individual antennas in a pair arise from gain differences in instrumentation chains; curves fitted to the points have the standard decade of time per 10-dB multipath slope in the deep-fade region. The curves fitted to the simultaneous fading points have the standard decade of time per 5-dB slope in the deep-fade region. Space-diversity reception at Lusk is effective (Fig. 15), which is a result that could not be predicted using present methods. Successful space-diversity operation at Wendover could be predicted beforehand by viewing the transmitting antenna at Lusk as a feed illuminating a large aperture (the double reflectors), since little fading would be generated on the short Lusk-to-reflectors leg.

The measured improvements at -35 dB, 50 at Wendover and 30 at Lusk, are larger than the calculated values of 40 and 16, respectively.

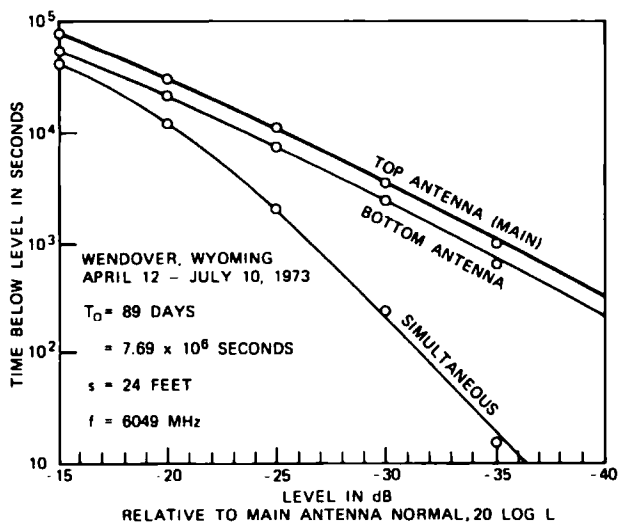


Fig. 14—Space diversity on path containing passive repeater; reception at Wendover, Wyoming.

The difference arises partly because use of the longest leg in the calculations is a simple approximation of a complex situation and partly because some scattering of measured points around the averages predicted by the equation for  $I_0$  can be expected.

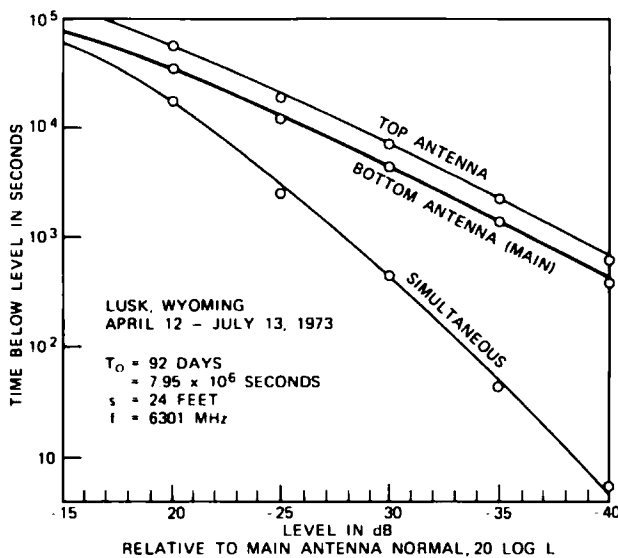


Fig. 15—Space diversity on path containing passive repeater; reception at Lusk, Wyoming.

**Table III — Parameters of Lusk Radio test—Lusk to  
Wendover, Wyoming**

Reflectors	Two 40- by 48-ft reflectors separated by 138.5 ft
Path lengths from reflectors: To Wendover To Lusk	31.5 miles 9.5 miles
Antenna separations at Wendover and Lusk	24 ft (nominal) vertical center to center
Frequencies: Wendover Lusk	6049 MHz received 6301 MHz received
Calculations: Values of $v^2$ arising from gain differences in instrumentation chains: Wendover Lusk Calculated improvement at -35 dB based on 31.5-mile path length Wendover ( $v^2 = 1.6$ ) Lusk ( $v^2 = 0.63$ ) Allocation to multipath fading from performance objectives for 41 miles (31.5 + 9.5)	$v^2 = 1.6$ $v^2 = 0.63$  $I_0 = 40$ $I_0 = 16$ $1600 \times 41/250 = 262$ seconds per year

The multipath objective for the Wendover-Lusk link is 262 seconds per year one way (see Table III). Even allowing the annual time below level to increase by a factor of two due to late summer and fall fading, the objective can be met comfortably with receiver fade margins in the 35- to 40-dB range.

#### **X. OVER-WATER PATHS**

Over-water paths, undesirable because of reflections, are sometimes unavoidable. When the over-water area is too large to permit shifting the reflection point off it via a high-low antenna combination, space diversity can be used to reduce reflection fading. A procedure for determining antenna spacing is discussed in terms of the geometry shown in Fig. 16, in which the reference plane coincides with the surface of the water during "flat-earth" propagation conditions (i.e., those obtaining when  $K$ , the ratio of equivalent to actual earth radius, is infinity). The "bulge" height  $h$  of the surface reflection point  $A$  is

$$h = d_1 d_2 / 1.5 K, \quad (14)$$

where  $h$  is in feet when  $d_1$  and  $d_2$  are in miles. If the height  $h_2$  of the receiving point were changed, then the relative phase of the rays arriving via the paths  $TR$  and  $TAR$  would also change. For a fixed

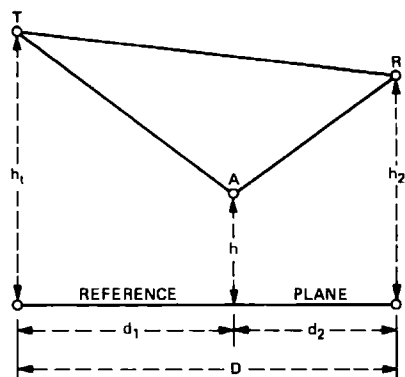


Fig. 16—Geometry for discussion of over-water paths.

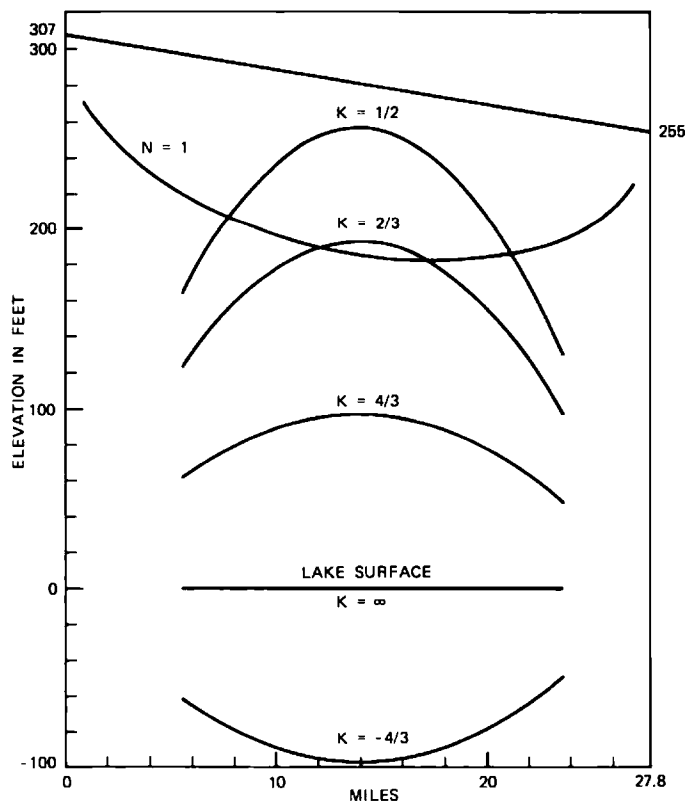


Fig. 17—Lake surface at various  $K$  values in over-water path example ( $N$  denotes boundary of  $N$ th Fresnel zone at a frequency of 4 GHz).

transmitting antenna height  $h_t$ , the increment in  $h_2$  for a change from an in-phase to an out-of-phase condition (half interference fringe spacing) is approximately (for large  $K$ ), in feet,

$$\Delta h_2 \approx 1300D/f(h_t - h), \quad (15)$$

where  $h_t$  and  $h$  are in feet,  $D$  is the path length in miles, and  $f$  is the frequency in GHz.

The desired antenna separation for good diversity, therefore, would be equal to  $\Delta h_2$ , but this is possible for one value of  $K$  only, since  $\Delta h_2$  increases as  $h$  increases (an increase of  $h$  results from a decrease of  $K$ ). For protection over a large range of  $K$ , a suitable initial choice for the antenna separation is

$$s = 1300D/fh_t, \quad (16)$$

which corresponds to  $\Delta h_2$  for  $K = \infty$ . The appropriateness of this

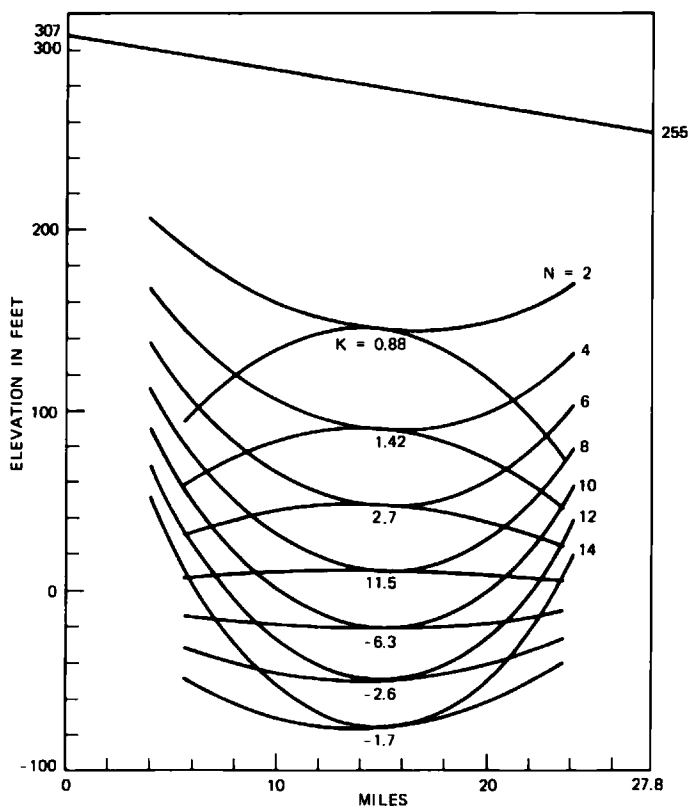


Fig. 18—Values of  $K$  at which lake surface is tangent to even Fresnel zone boundaries at a frequency of 4 GHz.

choice must be verified. In a recently examined situation (shown in Fig. 17) the path length  $D$  is 27.8 miles, the transmitting antenna height  $h_t$  is 307 feet, and the receiving antenna height  $h_r$  is 255 feet; since the planned hop is on the Gulf coast, the antennas are placed high to avoid obstruction fading. Protection from fading created by reflections from the lake surface is desired for values of  $K$  ranging from  $\frac{1}{2}$  to about  $-\frac{1}{3}$  (Fig. 17 and the subsequent drawings were generated very easily on an  $xy$ -plotter driven by a programmable desk calculator). Values of  $K$  for which the lake surface is tangent to even Fresnel zone boundaries (determined by trial and error) are shown in Fig. 18; at these values of  $K$ , signal minima occur at the 255-foot height. For 4-GHz transmission, a first choice for diversity antenna separation would place the second receiving antenna at the 225-foot height  $[(1300 \times 27.8)/(4 \times 307) \approx 30; 255 - 30 = 225]$ . Simultaneous sig-

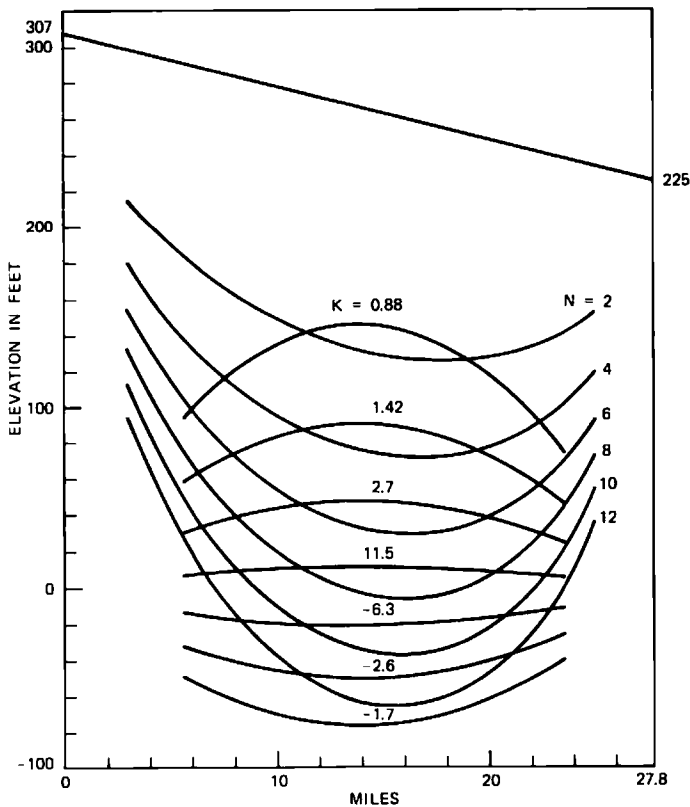


Fig. 19—Even Fresnel zone boundaries at 225-foot height for bottom receiving antenna at a frequency of 4 GHz.

nal minima will not occur on the two antennas because even Fresnel zone boundaries for the 225-foot height are not tangent to the lake surface at  $K$  values that correspond to signal minima on the top receiving antenna (see Fig. 19). The question of optimization now arises. It would be desirable to place the bottom antenna somewhat lower to move the boundary of  $F_2$  down, further away from the lake surface at  $K = 0.88$ ; this would bring the boundary of  $F_{12}$  closer to the lake surface at  $K = -1.7$  and, therefore, is not desirable. If the design requirements were relaxed to cover values of  $K$  between  $\frac{1}{2}$  and  $\infty$  only, then the bottom antenna could be brought further down to make the separation closer to the value of  $\Delta h_2$  at  $K = \frac{1}{2}$ .

A possible alternative location of the bottom antenna, foreground permitting, is the 85-foot height (see Fig. 20). This has some

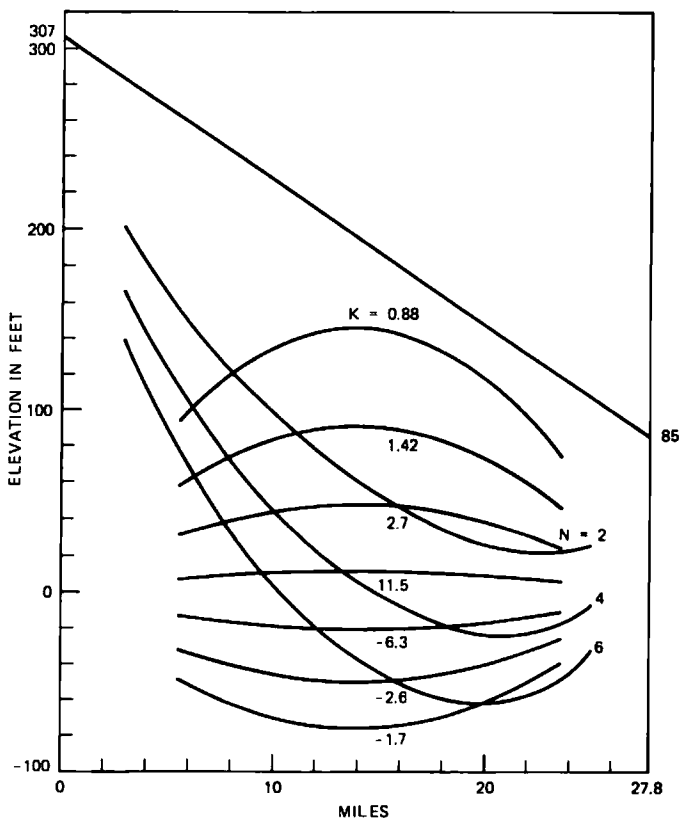


Fig. 20—Even Fresnel zone boundaries at 85-foot height for bottom receiving antenna at a frequency of 4 GHz.



of the properties of a high-low shot, and the even Fresnel zone boundaries are well placed.

A final observation on space-diversity design for protection from reflections is that the antenna spacings often are suitable, fortunately, for protection from atmospheric multipath fading.

## XI. CLEARANCE RULES

Operating experience indicates that propagation conditions in various sections of the United States can be classified, in broad terms, as good, average, or difficult as shown on the map in Fig. 21. Desired clearances for transmission between main antennas are summarized in Table IV. In addition, hop lengths in coastal areas of the southern United States are sometimes restricted to 20 miles to reduce obstruction fading.

Clearance requirements for antennas added to provide space-diversity protection from multipath fading are less stringent:  $0.6 F_1$  at  $K = \frac{4}{3}$ , with a foreground clearance of 10 feet in the first 500 feet from the antenna. In many cases, this permits placement of the secondary antenna below the main antenna.

It appears (from recent results discussed in Appendix A) that it may be possible to relax the secondary-antenna clearance require-

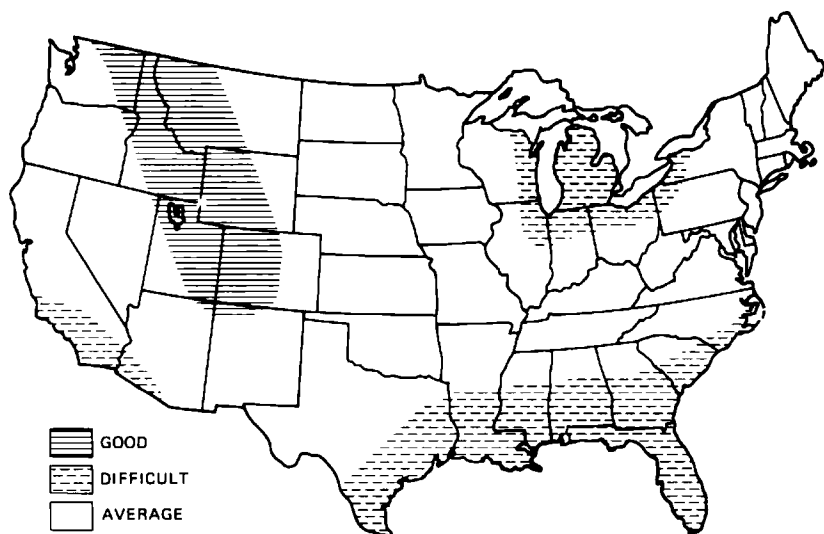


Fig. 21—Geographic occurrence of good, average, and difficult propagation conditions.

Table IV — Clearance rules for top antennas

Propagation Conditions	Clearance
Good Average Difficult	0.6 $F_1$ at $K = 1$ (but not less than grazing at $K = \frac{2}{3}$ ) The larger of 0.3 $F_1$ at $K = \frac{2}{3}$ and $F_1$ at $K = \frac{2}{3}$ Grazing at $K = \frac{2}{3}$

ments; however, results of further tests (now in progress) must be evaluated before general recommendations on this can be made.

## XII. ACKNOWLEDGMENTS

We are indebted to W. T. Barnett and E. E. Muller for useful discussions. The Multiple Input Data Acquisition System (MIDAS) and Portable Propagation Recorder (PPR) were designed by G. A. Zimmerman.

## APPENDIX A

### *Effects of Reduced Clearance*

The purpose of the bottom antenna in a space-diversity pair is to provide protection from multipath fading; its clearance therefore need not be based on requirements for protection from obstruction fading. Placement of secondary antennas lower than currently permitted would reduce tower costs because of reduced wind loading.

An investigation of multipath fading as a function of antenna height was undertaken at Palmetto, Georgia in 1972 at 4.198 GHz on a 26.4-mile path from Atlanta, Georgia.<sup>20</sup> The path profile (Fig. 22; arrows denote trees) shows that the controlling obstruction is located some 6 miles from the receiving antennas at Palmetto. Lines of sight that graze the obstruction are shown in Fig. 22 for three kinds of atmospheric conditions. Under normal conditions the gradient of the index of refraction is  $-39 N$  units per kilometer,\* and the ratio  $K$  of the equivalent-to-actual earth radius is  $\frac{4}{3}$ . When the gradient becomes  $-157 N$  units per kilometer, the so-called flat-earth condition exists ( $K = \infty$ ) and clearance is substantial. For changes of the gradient in the opposite direction, clearance becomes reduced; in path design the value of interest is  $K = \frac{2}{3}$ , which corresponds to a positive gradient of  $79 N$  units per kilometer.

The projections of the grazing lines on the Palmetto tower are given by the tops of the three bars on the right-hand side of Fig. 23, at 30,

\* The radio refractive index of air,  $n$ , is frequently expressed as  $n = 1 + N \times 10^6$ , where  $N$  describes the refractive index in "N units."

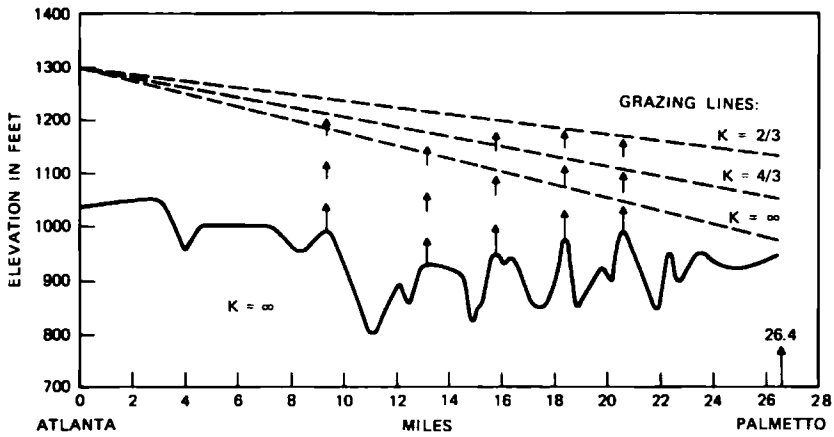


Fig. 22—Path profile, Atlanta to Palmetto, Georgia.

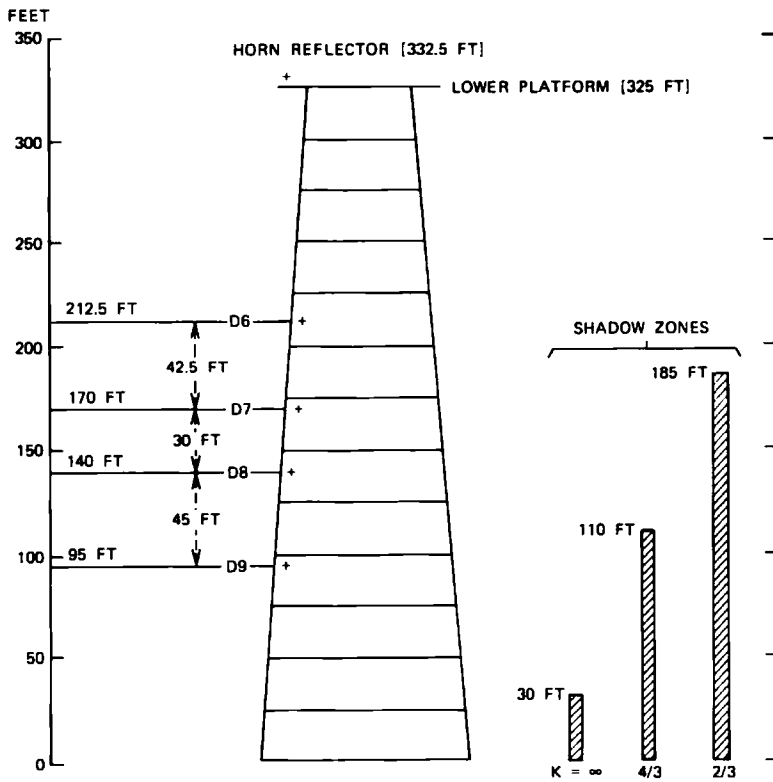


Fig. 23—Receiving antennas at Palmetto, Georgia in 1972.

110, and 185 feet from ground. The center line of the horn-reflector receiving antenna is 332.5 feet from ground. The center lines of the antennas added for test purposes are labeled D6 through D9. The antenna at D7 was a small 15-dB-gain horn; the other three are 4-foot-diameter parabolic reflectors. The normal antenna height for reception from Atlanta would be at about D6; the tower is much higher because clearance on another path controls its height.

The antenna of interest is the bottom 4-foot parabolic reflector at D9, with center line 95 feet above ground. The center line is 15 feet below the point where the grazing line under normal conditions ( $K = \frac{4}{3}$ ) projects on the tower. The clearance in Fresnel zones is about  $-0.2F_1$ . The center line of the bottom antenna falls on the grazing line when  $K$  is about 1.72, which corresponds to an index of refraction gradient of about  $-66 N$  units per kilometer, which is 27  $N$  units per kilometer higher than the gradient of  $-39 N$  units per kilometer under normal  $K = \frac{4}{3}$  conditions.

The below-grazing location of the bottom antenna was further verified by noting that there was a signal loss of 14 dB when it was moved from its previous (higher) location on March 14, 1972. A theoretical loss of about 8 dB would occur if the obstruction were a knife edge; diffraction over a tree-covered hilltop accounts for the additional 6-dB loss.

Data were analyzed on received power (recorded by MIDAS<sup>21</sup>) during time intervals containing deep fading (more than 20 dB) on any of the five receiving antennas in April, May, and June of 1972. The total of such time intervals was about 13 hours during which the amount of fading was similar for the top four antennas. The *a priori* expectation was that the bottom antenna would fade more, since its signal level during normal daytime conditions was 14 dB low because of a lack of clearance. The opposite occurred: the signal received by the bottom antenna faded *less* than signals received by the four upper antennas.

The measured time-below-level data (during the 13 hours of deep-fading activity) for the bottom antenna (D9) and the one above it (D8) are shown in Fig. 24 (fading on the other antennas, after adjustment for gain differences, was the same as that on D8). The single antenna curves have the normal slope (decade of time per 10 dB) for deep multipath fades. Time below level for the bottom antenna is smaller than that for D8 by about a factor of three in the deep-fade region.

Diversity performance of the combination of D8 and D9 was excellent. Simultaneous fades on the two antennas were never deeper than about 18 dB from normal (see Fig. 24).

These results relate to aspects of radio propagation not covered by previous experience or theory. Physically, the observations can per-

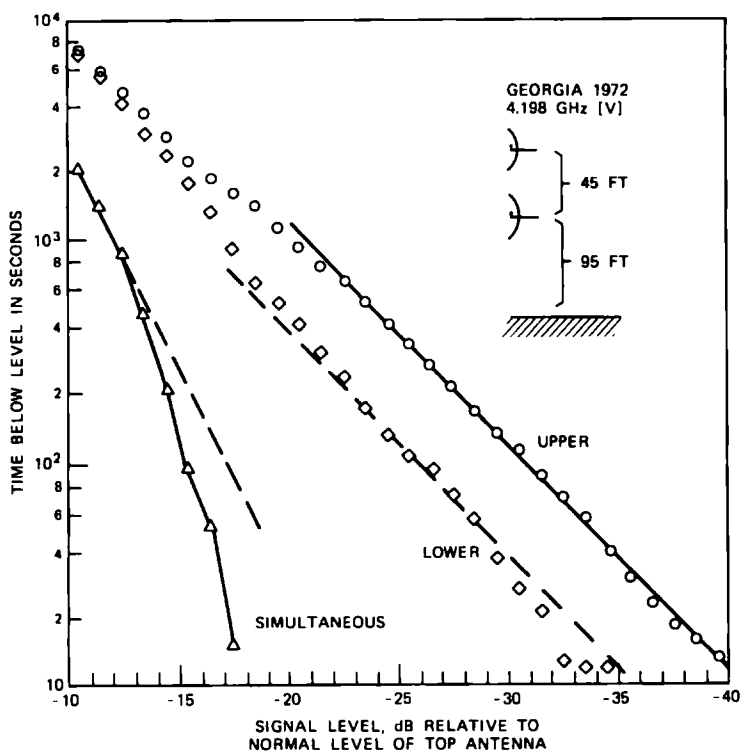


Fig. 24—Fading measured at Palmetto, Georgia.

haps be explained by the presence of layers with strong negative gradients in the index of refraction that create fading but offset the normal lack of clearance for the bottom antenna. Furthermore, since the bottom antenna is relatively close to the ground, the terrain blocks some of the potentially interfering rays, which would also tend to reduce the amount of fading.

A tentative conclusion is that protection from multipath fading can be obtained by placing the bottom antenna somewhat below grazing under normal atmospheric conditions (diffraction loss of perhaps 10 dB). It must be established that antennas placed in such a manner perform well consistently; results from tests at Culver, Indiana (1973–1974) are encouraging.

## APPENDIX B

### Example of Roughness Calculation

The terrain heights (denoted by  $x_i$ , terminal ends omitted) for the 19-mile path in the example of Fig. 25 are provided in Table V. The roughness (standard deviation) is the square root of the average

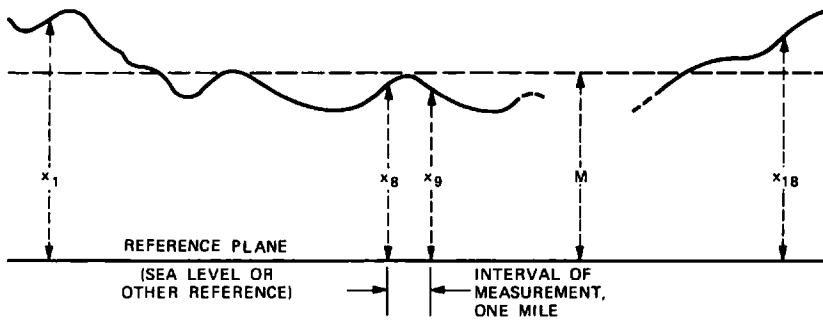


Fig. 25—Determination of terrain roughness.

Table V — Example of terrain heights for 19-mile path  
(see Fig. 25)

$i$	$x_i$ (ft)	$i$	$x_i$ (ft)	$i$	$x_i$ (ft)
1	600	7	400	13	450
2	625	8	420	14	420
3	515	9	460	15	390
4	440	10	420	16	480
5	480	11	450	17	520
6	450	12	480	18	550

square of the deviation from the mean:

$$\begin{aligned}
 w &= \sqrt{\frac{1}{18} \sum_{i=1}^{18} (x_i - M)^2} \\
 &= \sqrt{\left[ \frac{1}{18} \sum_{i=1}^{18} x_i^2 \right] - M^2} \quad (17)
 \end{aligned}$$

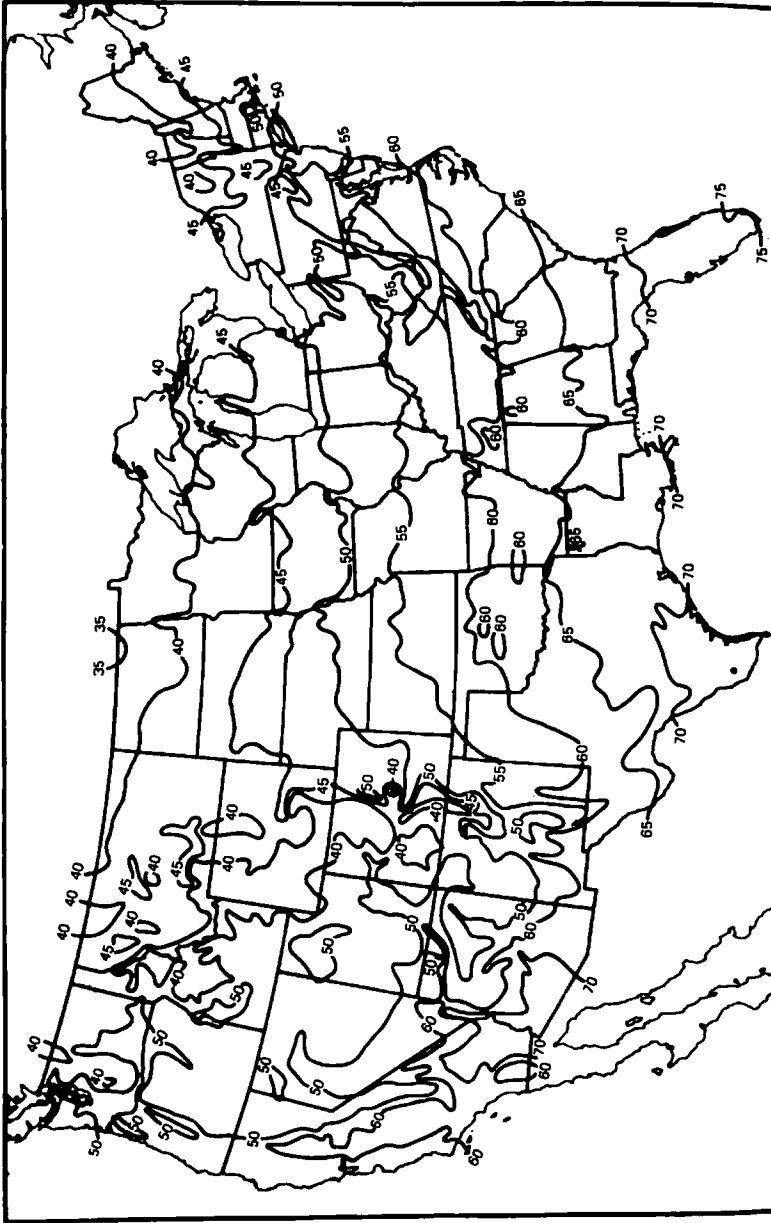
$$M = \frac{1}{18} \sum_{i=1}^{18} x_i = 8550/18 = 475 \quad (18)$$

$$w = \sqrt{(4133950/18) - (475)^2} = 63.5 \text{ feet.} \quad (19)$$

## APPENDIX C

### *Length of Fading Season*

Multipath fading is a warm-weather phenomenon. Assuming that the length of the warm portion of the year is proportional to the average annual temperature, the value of  $T_0$  to be used in eq. (2) to esti-



(Reprinted from the 1963 *Weather Handbook*, p. 194, by permission of the publisher, Conway Research, Inc., Atlanta, Georgia. No further reproduction is authorized.)  
Fig. 26—Average annual temperatures in °F.

mate the annual time below level is

$$T_0 = (t/50)8 \times 10^6 \text{ sec}, \quad 35 \leq t \leq 75, \quad (20)$$

where  $t$  denotes the average annual temperature of the locality in question in °F as determined from Fig. 26.

In the average case (Figs. 5 and 8),  $T_0$  is equal to the number of seconds in three months; eq. (20) reduces to this when  $t$  is 50°F. The temperature contours in Fig. 26 show that 50°F is appropriate for middle latitudes in the United States and for Ohio in particular; data from Ohio have often been used to describe average fading.

The range of average annual temperatures (Fig. 26) is from 35°F in northern North Dakota to 75°F in southern Florida. The corresponding fading season lengths range from 70 percent to 150 percent of average ( $T_0$  ranges from 2 months to  $4\frac{1}{2}$  months).

## APPENDIX D

### *Addition of Space Diversity to Frequency Diversity*

In the Bell System, fully loaded long-haul routes with radio channels in both the 4- and 6-GHz bands will utilize cross-band frequency-diversity protection with two protection channels—18 working channels in a  $2 \times 18$  system.<sup>14</sup> Expectations are that space diversity in  $2 \times 18$  protection systems will be needed only when problem hops are encountered—exceptionally high fading activity or unavoidable ground reflections—that will have to be treated on an individual basis. The need for space-diversity protection will arise on long-haul routes that have radio channels in one frequency band only, 4 or 6 GHz; the single frequency-diversity channel permitted on such routes<sup>1</sup> may not provide adequate protection in geographic areas where fading activity is above average.

The time below level at the fade margin of an average working channel in a frequency-diversity system with one protection channel and  $m$  working channels (a  $1 \times m$  system) is approximately equal to the simultaneous time below level of channels in an equivalent  $1 \times 1$  system in which the separation of the center frequencies of the two channels is

$$\Delta f_{eq} = m / \left[ \sum_k (1/\Delta f_k) \right], \quad (21)$$

where the sum contains  $\frac{1}{2}m(m+1)$  terms, extending the summation over frequency separations of all channel pairs in the  $1 \times m$  system. The equivalent  $1 \times 1$  system (introduced to simplify calculations) is derived from the first term in the alternating series describing transmission unavailability<sup>14</sup> under the assumption that equipment works



perfectly during fading (equipment failures are accounted for via the allocation of transmission availability objectives).

The simultaneous time below level of the two channels in the equivalent  $1 \times 1$  system is

$$T_{eq} = T/I_{eq}, \quad (22)$$

where  $T$  is the time below level in an unprotected channel and

$$I_{eq} = q_{eq}L^{-2}, \quad (23)$$

with  $q_{eq}$  determined by using  $\Delta f_{eq}$  in eq. (10). As an example, in a  $1 \times 3$  system with 60 MHz between channels

$$\begin{aligned} \Delta f_{eq} &= \frac{3}{(3/60) + (2/120) + (1/180)} \\ &= 41.5 \text{ MHz.} \end{aligned} \quad (24)$$

Similarly, in a  $1 \times 7$  system with 30 MHz between channels,

$$\Delta f_{eq} = 15.3 \text{ MHz.} \quad (25)$$

The use of these values of  $\Delta f_{eq}$  to calculate  $T_{eq}$  for one hop is illustrated in the example in Table VI and Fig. 27. In a multihop switching section,  $T_{eq}$  would be determined by adding values of  $T_{eq}$  determined for each hop.

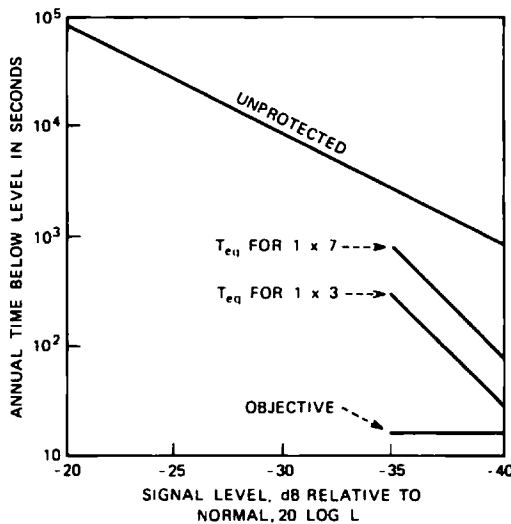


Fig. 27—Example of need for space-diversity protection (see Table VI for path parameters and calculations).

Table VI — Sample calculations

Path parameters	$D = 20$ miles (southern coastal area) $f = 6$ GHz $w = 20$ feet $t = 70^\circ\text{F}$
Fading in an unprotected channel	$c = 2(w/50)^{-1.2} = 6.58$ $r = c(f/4)D^{1.5}10^{-4} = 0.79$ $T_0 = (t/50)8 \times 10^4 = 1.12 \times 10^7$ seconds $T = rT_0L^2 = 8.8 \times 10^4 L^2$ seconds/year
Long-haul objective	$1600 \times D/2000 = 16$ seconds/year
Equivalent $1 \times 1$ system replacing $1 \times 3$	$\Delta f_{eq} = 41.5$ MHz $q_{eq} = (50/6 \times 20) \times (41.5/6000) = 0.0029$ $I_{eq} = 0.0029 L^{-2}$
Equivalent $1 \times 1$ system replacing $1 \times 7$	$\Delta f_{eq} = 15.3$ MHz $q_{eq} = (50/6 \times 20) \times (15.3/6000) = 0.0011$ $I_{eq} = 0.0011 L^{-2}$

The long-haul objective (using  $D_s$  to denote the length of the switching section) is

$$T_{ob} = 1600D_s/2000 \text{ sec}, \quad (26)$$

in terms of which the recommendations for the application of space diversity are:

$$T_{eq} < T_{ob}, \text{ space diversity not needed}, \quad (27)$$

$$T_{eq} > 1.5 T_{ob}, \text{ space diversity needed}. \quad (28)$$

Use of space diversity is optional in the tolerance band ( $T_{ob} \leq T_{eq} \leq 1.5 T_{ob}$ ), which reflects parameter uncertainties and the fact that the approximation used to determine  $T_{eq}$  overestimates the unavailability. According to the above criteria, space diversity is needed in the example in Fig. 27 (assuming a one-hop switching section with 40-dB fade margin).

If space-diversity protection is needed, then it should first be applied to the worst hop in a switching section. In subsequent calculations,  $T_s$  from eq. (6) should replace  $T_{eq}$  for space-diversity-equipped hops, since improvement due to space diversity is normally dominant.

## APPENDIX E

### Comparative Switching With Hysteresis

The analysis is carried out in terms of the envelope voltages ( $R_1$  and  $R_2$ ) of the signals from the two receiving antennas. The antennas are

assumed to be of the same size and  $R_1$  and  $R_2$  are normalized to be unity in the absence of fading. The envelope  $R$  of the diversity signal is a composite of  $R_1$  and  $R_2$  obtained by switching;  $R$  becomes  $R_1$  when  $R_1 > bR_2$  and  $R$  becomes  $R_2$  when  $R_2 > bR_1$ . The parameter  $b$  ( $b \geq 1$ ) describes the hysteresis of the switch.

The probability of a fade of  $20 \log L$  dB is the probability that  $R < L$ . Regions in the  $R_1, R_2$ -plane over which the joint probability density function  $p(R_1, R_2)$  has to be integrated to obtain this probability are shown in Fig. 28. This shows that

$$\begin{aligned} \Pr(R < L) = & \int_0^L dR_2 \int_0^L dR_1 p(R_1, R_2) + \frac{1}{2} \int dR_2 \int dR_1 p(R_1, R_2) \\ & \text{over triangle 1,} \\ & + \frac{1}{2} \int dR_2 \int dR_1 p(R_1, R_2) \\ & \text{over triangle 2.} \end{aligned} \quad (29)$$

For deep fades and antennas of equal size,<sup>8</sup>

$$p(R_1, R_2) \cong 4q^{-1}R_1R_2. \quad (30)$$

Substitution and integration gives

$$\Pr(R < L) \cong q^{-1}L^4 \frac{b^2 + b^{-2}}{2}. \quad (31)$$

In the absence of hysteresis,  $b$  is unity. When hysteresis is introduced,  $b$  becomes larger than unity, and the probability of fading is increased by a factor of  $0.5(b^2 + b^{-2})$ .

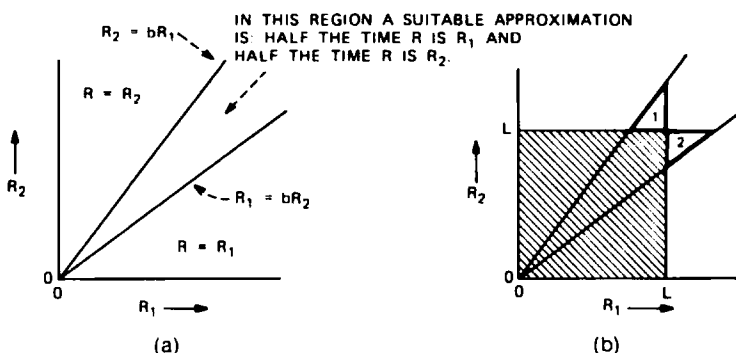


Fig. 28—Comparative switching with hysteresis. (a) Switching diagram. (b) Areas in which  $R < L$ .

## APPENDIX F

### Threshold Switching Calculations

Below threshold the switch cycles, and  $R$  is  $R_1$  or  $R_2$  in equal amounts of time; the below-level probability for below-threshold operation is, with  $A$  denoting the threshold value,

$$\Pr(R < L) = \frac{1}{2} \Pr(R_1 < L, R_2 < A) + \frac{1}{2} \Pr(R_1 < A, R_2 < L), L < A. \quad (32)$$

Because of symmetry in the joint probability density function, this simplifies to

$$\Pr(R < L) = \int_0^L dR_1 \int_0^A dR_2 p(R_1, R_2), \quad L < A \quad (33)$$

for antennas of equal size. The below-level probability in above-threshold operation is (invoking symmetry as above) the sum of two terms. The first term describes the situation when  $R$  is  $R_1$ , the second when  $R$  has become  $R_2$  upon  $R_1$  dropping below threshold:

$$\Pr(R < L) = \Pr(A < R_1 < L) + \Pr(R_1 < A, R_2 < L), \quad L > A. \quad (34)$$

These equations are based on results obtained for correlated Rayleigh distributed variables.<sup>2</sup> Use of the probability density function from eq. (30) in (33) gives a deep fade approximation:

$$\Pr(R < L) \cong q^{-1} A^2 L^2, \quad L < A, \quad (35)$$

which shows the  $L^2$  behavior below threshold.

The curves in Figs. 10 and 11 were calculated (as outlined above) for correlated Rayleigh-distributed variables with  $q$  determined from the empirical expression for  $I_0$  (machine computation was necessary because the integrals cannot be evaluated in closed form). The Rayleigh distribution was used in the theoretical calculations because its previous uses have provided insights valuable to the statistical description of space-diversity operation. The theoretically predicted functional forms have been verified by using actual fading records as inputs to computer-simulated threshold switches.<sup>22</sup>

## APPENDIX G

### Common Control Switching

Space-diversity switching is normally implemented on a per-channel basis: each radio channel has its own switch, and switching decisions for a channel are based, in FM systems, on carrier levels received on

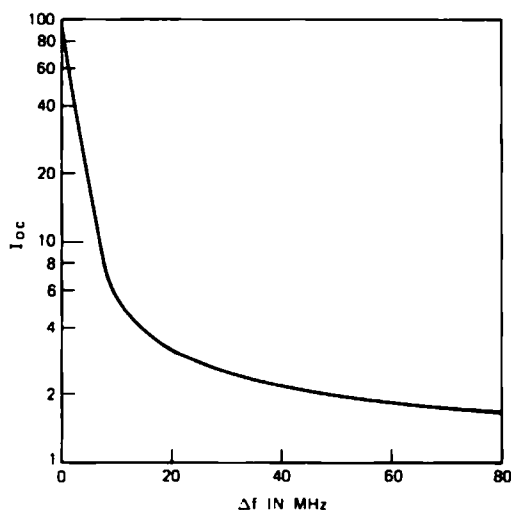


Fig. 29—Improvement in a controlled channel as a function of frequency separation from controlling channel (4-GHz band, 30-foot antenna separation, 26-mile path, 40-dB fade margin).

the upper and lower antennas. Use of the carrier in one channel (controlling channel) to control switching of other channels (controlled channels) would reduce costs. For example, diversity transmission could be controlled by the received carrier in another channel, thus eliminating the feedback link; similarly, a single broadband switch could be used to switch a number of radio channels. Unfortunately, the improvement obtained in such common control schemes is too small to be of practical value.

The available improvement  $I_{oc}$  in a controlled channel depends on  $\Delta f$ , the frequency separation of the carriers in the controlling and controlled channels. When  $\Delta f$  is zero,  $I_{oc}$  is equal to the available improvement  $I_0$  in the controlling channel, with  $I_0$  given by (7). In the limit, as  $\Delta f$  increases and becomes large,  $I_{oc}$  approaches unity as fading at the two frequencies becomes independent. Theoretical estimates<sup>23</sup> show that the initial decrease in  $I_{oc}$  as  $\Delta f$  increases from zero is rapid. As an example, the approximate behavior of  $I_{oc}$  as a function of  $\Delta f$  in the 4-GHz band is shown in Fig. 29 for a 30-foot antenna separation on a 26-mile path and with a fade margin of 40 dB. The value of  $I_{oc}$  at  $\Delta f = 0$  is about 100. At one channel separation,  $\Delta f = 20$  MHz,  $I_{oc}$  has decreased to about 3. Clearly, the improvement in the controlled channels is too small to be of practical value. The lack of performance in common control switching is simply a consequence of the fact that deep multipath fades are highly frequency selective.

## APPENDIX H

### Results of Palmetto, Georgia, Experiments in 1968

Power received at 4.198 GHz on five vertically separated antennas (Fig. 30) was measured on a 24.6-mile path from Atlanta to Palmetto, Georgia over a 72-day period in 1968 (August 16–October 27). Five inputs of MIDAS<sup>21</sup> (Multiple Input Data Acquisition System) were used to acquire the data. A power reading from the horn reflector on top was obtained first; about 2 milliseconds later, a reading from the top dish was obtained, and so on down the tower. This scanning was repeated at a rate of five times per second. The readings were converted to a logarithmic scale and recorded in digital form (nominally 1 dB quantizing) on magnetic tape for subsequent computer processing. In the absence of fading, to conserve tape, the recording rate was less than the sampling rate.

Improvement as a function of fade depth for the ten antenna pairs, with separations ranging from 4 to 60 feet center-to-center, was obtained by dividing at a given fade depth the measured time below level for an antenna ( $T$ ) by the measured simultaneous time below level ( $T_*$ ). The equation for improvement,

$$I_0 = qL^{-2}, \quad (36)$$

was fitted to the points in the deep-fade region to determine a value of  $q$  for each antenna separation ( $v^2 = 1$ , since gains were set to equalize free-space levels). The values of  $q$  so obtained are shown in Fig. 31 as a function of antenna separation; because of random differences in

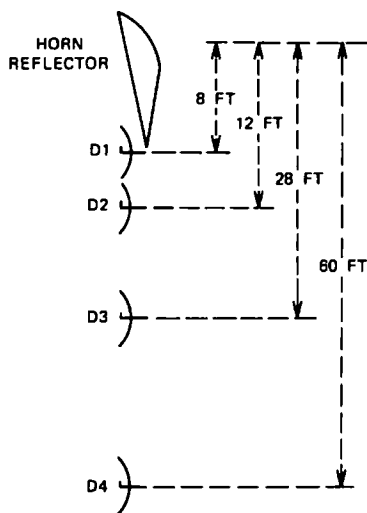


Fig. 30—Receiving antennas at Palmetto, Georgia in 1968. D1 to D4 are 4-foot-diameter parabolic reflectors.

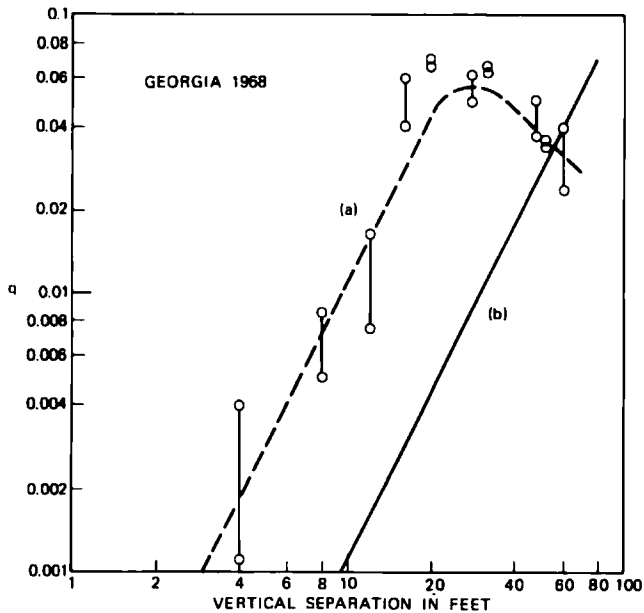


Fig. 31—Variation of correlation parameter  $q$ : (a) Georgia 1968, and (b) eq. (9). Increasing values of  $q$  denote increasing decorrelation.

$T$  from antenna to antenna, there are two values of  $q$  for each antenna separation, depending on whether  $T$  for the upper or the lower antenna was used to form the ratio  $T/T_*$ .

As a function of antenna separation, the correlation parameter  $q$  first increases as the square of the antenna separation, but then levels off and decreases (dotted line in Fig. 31); the presence of a small dominant component in the multipath spectrum is the most likely cause of this. Compared to eq. (9) (see also solid line in Fig. 31),  $q$  is enhanced for smaller separations, but is reduced for separations over about 50 feet. Dominant components being random on paths designed for negligible ground reflections, the enhancement cannot be counted upon when choosing an antenna separation; however, the possibility that  $q$  may decrease for large separations must be provided for. This is the reason why the applicability (for design purposes) of (7) has been limited to antenna separations of 50 feet or less.

## REFERENCES

1. FCC First Report and Order (Docket 18920), June 3, 1971.
2. E. Henze, "Theoretische Untersuchungen über einige Diversity-Verfahren," *Archiv Elektrischen Übertragung*, 11, No. 5 (May 1957), pp. 183-194.
3. H. Makino and K. Morita, "The Space Diversity Reception and Transmission Systems for Line-of-Sight Microwave Link," *Rev. Elec. Comm. Lab (Japan)*, 13, No. 1-2 (January-February 1965), pp. 111-129.

4. H. Makino and K. Morita, "Design of Space Diversity Receiving and Transmitting Systems for Line-of-Sight Microwave Links," *IEEE Trans. Commun. Tech.*, *COM-15*, No. 4 (August 1967), pp. 603-614.
5. R. F. White, "Space Diversity on Line-of-Sight Microwave Systems," *IEEE Trans. Commun. Tech.*, *COM-16*, No. 1 (February 1968), pp. 119-133.
6. R. F. White, *Engineering Considerations for Microwave Communications Systems*, San Carlos, Calif.: Lenkurt Electric Co., June 1970.
7. A. Vigants, "Space-Diversity Performance as a Function of Antenna Separation," *IEEE Trans. Commun. Tech.*, *COM-16*, No. 6 (December 1968), pp. 831-836.
8. A. Vigants, "The Number of Fades in Space-Diversity Reception," *B.S.T.J.*, *49*, No. 7 (September 1970), pp. 1513-1530.
9. W. T. Barnett, "Multipath Propagation at 4, 6, and 11 GHz," *B.S.T.J.*, *51*, No. 2 (February 1972), pp. 321-361.
10. S. H. Lin, "Statistical Behavior of a Fading Signal," *B.S.T.J.*, *50*, No. 10 (December 1971), pp. 3211-3270.
11. A. Vigants, "Number and Duration of Fades at 6 and 4 GHz," *B.S.T.J.*, *50*, No. 3 (March 1971), pp. 815-841.
12. K. W. Pearson, "Method for the Prediction of the Fading Performance of a Multisection Microwave Link," *Proc. IEE (London)*, *112*, No. 7 (July 1965), pp. 1291-1300.
13. A. Vigants, "Observations of 4 GHz Obstruction Fading," *Proc. IEEE Int. Conf. on Commun.*, *8*, 1972, pp. 28-1 to 28-2.
14. W. Y. S. Chen, "Estimated Outage in Long-Haul Radio Relay Systems with Protection Switching," *B.S.T.J.*, *50*, No. 4 (April 1971), pp. 1455-1485.
15. S. H. Lin, "Statistical Behavior of Deep Fade of Diversity Signals," *IEEE Trans. Commun.*, *COM-20*, No. 6 (December 1972), pp. 1100-1107.
16. W. T. Barnett, unpublished work.
17. W. T. Barnett, unpublished work.
18. A. Vigants, "Threshold-Switched LOS Space-Diversity Reception in the Everglades," *Conf. Record*, pages 12C-1 to 12C-3, *IEEE Int. Conf. Commun.*, June 17-19, 1974 Minneapolis, Minnesota; Institute of Electrical and Electronics Engineers, 1974.
19. A. Vigants, "Space Diversity on a 6-GHz Path with Billboard Reflectors," *Conference Record*, pages 12B-1 to 12B-4, *International Conference on Communications*, June 17-19, 1974, Minneapolis, Minnesota; Institute of Electrical and Electronics Engineers, 1974.
20. A. Vigants, "Variation of Fading with Antenna Height and Size," *URSI/IEEE G-AP Int. Symp.*, Williamsburg, Va., December 11-15, 1972.
21. K. Bullington, "Unlocking the Secrets of Microwave Propagation," *Bell Laboratories Record*, *50*, No. 1 (January 1972), pp. 8-13.
22. M. V. Pursley, unpublished work.
23. A. Vigants, unpublished work.